

Avalanche dynamics in driven materials

Jordi Baró¹, Antoni Planes¹, Eduard Vives^{1,2*}

¹Departament de Física de la Matèria Condensada, Universitat de Barcelona, Barcelona, Catalonia. ²Universitat de Barcelona Institute of Complex Systems (UBICS), Universitat de Barcelona, Barcelona, Catalonia

Summary. Phase transitions in equilibrium have traditionally been classified as first-order or second-order (critical). The essential difference between the two is whether the order parameter exhibits a discontinuous or a continuous behavior at the transition point. In the second half of the last century, second-order phase transitions were extensively studied. Concepts such as the lack of characteristic scales, divergence of correlation length, criticality, critical exponents, and universality were established. Very powerful techniques, such as the renormalization group approach, were developed as well. In the last 20 years, the focus has been on first-order phase transitions (FOPTs). Theoretically, systems slowly driven across a FOPT exhibit an equilibrium behavior with a single discontinuity of the order parameter. However, even when driven very slowly, they often evolve following a non-equilibrium metastable trajectory. This trajectory, instead of consisting of a single macroscopic discontinuity, exhibits many small discontinuities, or “avalanches,” with sizes ranging from the microscopic to the macroscopic. This behavior is an example of the “avalanche dynamics” discussed herein. The essential difference that distinguishes this behavior from other non-equilibrium intermittent dynamics is the lack of characteristic scales. This is why the term “critical” is applied to these systems, despite the fact that they undergo a FOPT. For this phenomenon to occur, two ingredients are needed: quenched-in disorder and athermal behavior, a consequence of low thermal fluctuations. However, “avalanche dynamics” is not limited to systems with FOPTs but may also occur in heterogeneous systems irreversibly driven by an instability. A second example discussed in this article is the case of the mechanical failure of porous materials under compression, for which disorder and athermal behavior play crucial roles. [*Contrib Sci* 11(2): 153-162 (2015)]

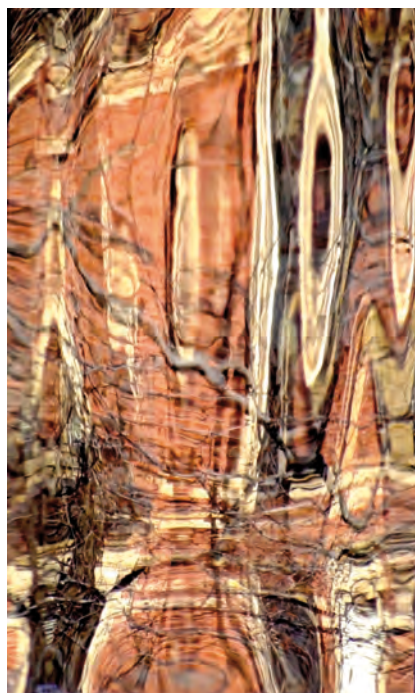
***Correspondence:**

Eduard Vives
Departament de Física de la Matèria
Condensada
Universitat de Barcelona
Martí i Franquès, 1
08028 Barcelona, Catalonia
Tel. +34-934021586
E-mail: eduard@ecm.ub.edu

Matter is organized as structures with different properties on both the macroscopic and the mesoscopic scale, the so-called phases. The relevant macroscopic properties are typically measured by extensive thermodynamic variables, such as volume (V), magnetization (M), polarization (P), and strain (ϵ).

A phase transition consists of a microscopic reorganization that alters some of these macroscopic properties of matter [12,23]. This reorganization can be interpreted as competition between three terms: internal energy (U), entropy (S), and the energy due to external forces. The three terms de-

Keywords: non-equilibrium first-order phase transitions · metastable behavior · hysteresis · avalanche dynamics · compression of porous materials



fine the Gibbs free energy (G). For instance, for a system that interacts with the surroundings only through hydrostatic pressure (p) and temperature (T), G can be written as:

$$G = U - TS - (-pV) \quad (1)$$

In general, there can be many terms like the one defined by Eq. (1), which is related to the work performed by external forces. Such terms are always written as the product of an intensive variable, whether pressure ($-p$), magnetic field (H), electric field (E), or stress (σ), and its conjugated extensive variable, i.e.: ($-pV$), HM , EP , or $\sigma\varepsilon$. Under slowly changing external conditions, systems relax to the equilibrium state, at which G is at an absolute minimum. For instance, an increase of T (at constant p) may cause the system to choose a state with higher entropy (S) and lower internal energy (U). These changes usually lead to a smooth response of the system, except at first-order phase transitions (FOPTs), as in the case of liquid–vapor phase transitions, in which entropy, energy, and volume undergo a sharp macroscopic change (related to the exchange of latent heat).

A second example is an increase of p at constant T , which may cause the system to choose a state with a lower volume (V) and lower entropy (S), as occurs abruptly during condensation. Therefore, FOPTs can be induced by changes in temperature or external forces. FOPTs are also seen in the singular behavior of thermodynamic response functions related to derivatives of extensive properties: specific heat (dU/dT), compressibility (dV/dT), susceptibilities (dM/dH and dP/dE), and elastic moduli ($d\varepsilon/d\sigma$).

FOPTs are widespread in nature. Some are very familiar, such as the freezing and boiling of water; others are related to changes in the crystallographic structure of solids or to the magnetic field induced magnetization switching of iron (below a given temperature, referred to as the Curie temperature, T_c). Some phase transitions involve more exotic properties, such as superconductivity or superfluidity.

Future technological innovation will require an understanding of both natural and man-made materials and of the methods to achieve their control. The development of increasingly smaller sensors and actuators awaits detailed knowledge of the equilibrium and out-of-equilibrium behaviors of materials driven by external forces and fields. Materials that respond with large variations in their order parameter when driven by relatively small forces are precisely those that exhibit a FOPT. Historically, the first motors were based on the expansion and contraction of gases. Nevertheless, motors only became truly powerful when the liquid-vapor

FOPT was exploited in the steam engine. Similarly, today's sensors and actuators are designed using ferroic or multiferroic materials involving FOPTs. Thus, both knowledge of the discontinuous dynamics of these systems during the transition and the ability to control this process are of extreme importance in the development of applications.

Landau theory of FOPTs

A simple framework that provides an understanding of the occurrence of FOPTs is the Landau theory [10]. It also provides a basic description of the hysteretic behavior of athermal systems and of the occurrence of avalanche dynamics in disordered-athermal systems. The theory was originally developed for continuous phase transitions but it was soon realized that, in some cases, it was also suitable to describe FOPTs. Firstly, the relevant order parameter for the transition, i.e., the extensive variable that exhibits macroscopic discontinuity, must be identified. Secondly, the free energy must be expanded in power series in the order parameter, including only the terms allowed by the symmetry of the problem. As an example, the case of a uniaxial ferromagnet under an applied external field is shown in Fig. 1. The two intensive control variables are the temperature (T) and the external field along the z-axis (H). Here, the order parameter is the magnetization (M), which exhibits a discontinuity at the transition, below the Curie temperature (T_c). The phase diagram (Fig. 1, left) shows a FOPT (dashed line) exactly at $H = 0$. Due to symmetry reasons, the two ferromagnetic phases, with $M > 0$ and $M < 0$, are completely equivalent when subjected to an inversion operation. The FOPT line ends at the critical point, at T_c . Let us assume that we drive the system at low enough temperatures, by changing H from a very large to a very low value, as indicated by the blue arrow in the phase diagram of Fig. 1.

The expansion of the Gibbs energy in terms of the magnetization will be:

$$G(M) = AM^2 + bM^4 + \dots - HM \quad (2)$$

Note that, taking into account symmetry considerations, in Eq. (2) only even terms are allowed, except for the term $-HM$ already discussed in the previous section. This is because symmetry between the two ferromagnetic phases is broken in the presence of an external field. In general, the coefficients in the expansion A , b ... depend on temperature. To a first approximation these dependences can be ig-

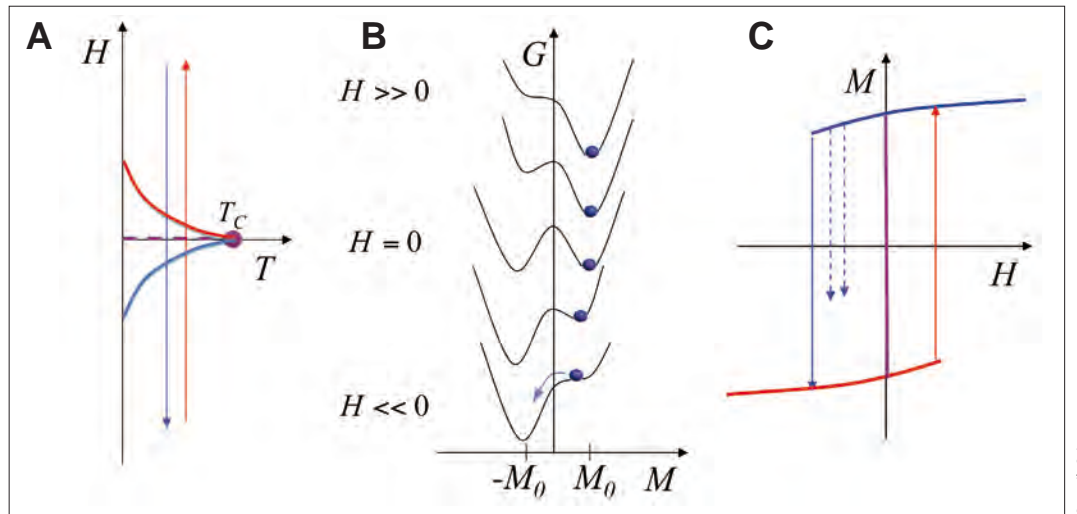


Fig. 1. (A) Schematic representation of the phase diagram of a uniaxial ferromagnet under athermal conditions. The dashed line is the equilibrium first-order phase transition (FOPT); the continuous lines indicate the metastability limits, in which the transition occurs in the perfectly athermal case. The two colors (blue and red) correspond to the two directions of the field variation: from $+\infty$ to $-\infty$ (blue) or from $-\infty$ to $+\infty$ (red). (B) Free energy $[G(M)]$ for different field values as indicated by the legend. The blue dot represents the metastable evolution of the system when the field is changed from $+\infty$ to $-\infty$. (C) Magnetization vs. field $[M(H)]$, in which hysteresis depends on the direction of the field variation. The dashed lines indicate the position of the jumps when a certain degree of thermal fluctuations is allowed.

Contrib Sci

nored, except for parameter A . This first term in the expansion is expected to vary rapidly near the critical temperature T_c . Its dependence on temperature is usually assumed to be of the form:

$$A = a(T - T_c) \quad (3)$$

Note that in Eq. (3), A vanishes exactly at T_c ; it is negative for $T < T_c$ and positive for $T > T_c$.

The panel in the center of Fig. 1 shows the behavior of the Landau free energy $[G(M)]$ for values of the field (H) that range from very large and positive (Fig. 1, top) to very large and negative (Fig. 1, bottom). Note the existence of two wells precisely due to the fact that $T < T_c$ and A is negative. Above T_c ($A > 0$), the Landau free energy will exhibit a unique well and the FOPT will not occur. Note also that the effect of the external field [given by the last linear term in the expansion (HM)] is simply to tilt the double-well function.

As explained in the Introduction, the system chooses the equilibrium state that corresponds to the global minimum of $G(M)$. For positive fields the equilibrium value of M will correspond to the well on the right hand side ($M > 0$) and for negative fields to the well on the left hand side ($M < 0$). At $H = 0$, the two wells have the same depth at symmetric positions $\pm M_0$. The system will therefore display a discontinuous change of magnetization ($\Delta M = 2M_0$) as the field

moves from positive to negative values.

The panel on the right in Fig. 1 shows the corresponding behavior of the magnetization as discussed. The equilibrium trajectory is shown by a thick line, displaying the discontinuity at $H = 0$. At exactly $H = 0$, the two phases (corresponding to the two symmetric wells) will coexist, giving rise to a heterogeneous microstructure. This simple version of the Landau theory cannot provide a detailed description of the coexisting state. The details will be determined by the system's shape and surfaces and by interaction terms such as those of demagnetizing fields (in ferromagnets) or elastic forces (in ferroelastics).

An important factor that must be taken into account in order to understand avalanche dynamics is the role of thermal fluctuations. For a system to follow an equilibrium trajectory, microscopic thermal fluctuations are needed because they allow temporal and spatial deviations of the energy from its exact value at the minimum. The system, therefore, is able to explore the phase space and jump over energetic barriers. This ability is essential in the vicinity of a FOPT for the system to abandon a local minimum and jump into a global minimum. This can be understood from the central panel in Fig. 1. As soon as the field (H) becomes infinitesimally negative, the system should jump towards the well on the left hand side.

There are several scenarios in which thermal fluctuations

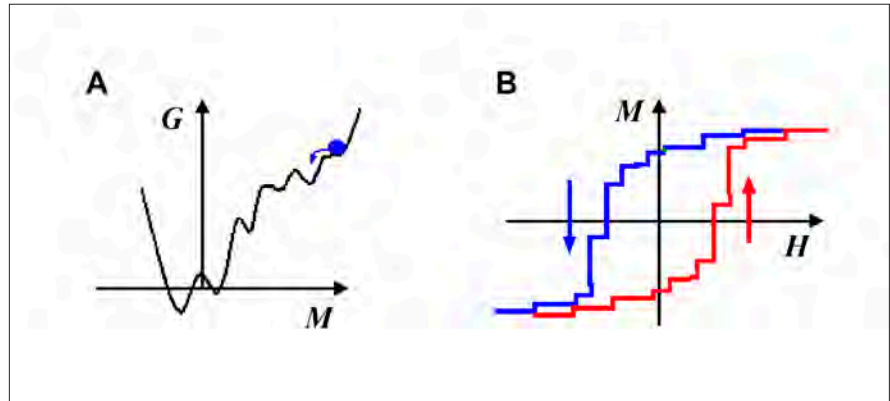


Fig. 2. (A) Schematic representation of the free energy $G(M)$ for a system with a FOPT and quenched disorder. (B) Corresponding hysteresis loops exhibiting avalanches associated with the jumps from one metastable minimum to the next.

become irrelevant. In some cases the reasons are kinetic: the system is externally driven very rapidly compared to the time needed to explore the phase space. In other cases, the existence of long-range forces (of an elastic, magnetic, or electrical nature) may enormously increase the size of the energetic barriers separating the minima of the free energy. In both cases the consequence is that the system will not follow an equilibrium path and will remain trapped in local (metastable) minima, as shown by the blue dots in the central panel of Fig. 1. This gives rise to hysteretic (out-of-equilibrium) behavior [3], an effect well known to occur in many FOPTs. For instance, liquid water at atmospheric pressure may become undercooled below 0°C and freeze (phase change) at much lower temperatures. The right-hand panel in Fig. 1 also shows the trajectories that the system will follow in the case of its having a completely athermal character (thin continuous lines with arrows). In this case, the transition to the absolute minimum only occurs when the local minima disappear. Note that the transitions occur at values of the field (H) that depend on whether the field is increased or decreased. The difference between these two fields provides a measure of hysteresis.

In general, if the athermal character is not strictly ideal, the system may display the transition when the local minimum is shallow enough. In this case hysteresis will depend on the rate at which the external field is driven (dashed lines in the right-hand panel of Fig. 1). In the ideal athermal case, hysteresis becomes rate independent. In the phase diagram, the transitions will not occur when the equilibrium FOPT line at $H = 0$ is crossed but, instead, when the so-called metastability limits are exceeded. In the left-hand panel in Fig. 1, the continuous blue and red lines show the metastability limits corresponding to trajectories that decrease or increase the field, respectively.

We now discuss the role of the second factor that is need-

ed for avalanche dynamics to occur: disorder. Real materials are never perfect. Even crystals exhibit inhomogeneities in the form of dislocations, vacancies, lack of stoichiometry, and impurities. One of the consequences of disorder is that the free energy landscape of the system is much more complex than the free energy in the case of only two wells, as depicted in Fig. 1. Different parts of the system may exhibit different degrees of metastability with correspondingly different values of the local magnetizations. Of course, under these conditions, the correct description of the system cannot be provided with a free energy function of a simple scalar order parameter such as the magnetization (M), but requires a description using a functional of an order parameter field $[m(x)]$, such that its integral over the whole system volume gives M . The free energy functional will then include terms coupling the local disorder with $m(x)$. Nevertheless, for the purpose of simplicity, such as the example in the central panel of Fig. 1 we project the free energy functional into a function of the average magnetization ($\langle M \rangle$). Therefore, the consequence of the existence of inhomogeneities is that the free energy displays multiple small wells separated by free energy barriers between the two phases with positive and negative magnetization, as shown in the left-hand panel of Fig. 2.

If we now combine both the athermal behavior and the existence of disorder, the metastable trajectory of the system will consist of a series of small jumps which take place every time the system relaxes from a local metastable minimum and falls into a new one. A schematic representation is shown in the right-hand panel of Fig. 2. These jumps are avalanches. Their characteristic property is that, even if the system is driven very smoothly, the response of the system to the applied field is intermittent, in which periods without activity alternate with periods characterized by very fast changes in the order parameter.

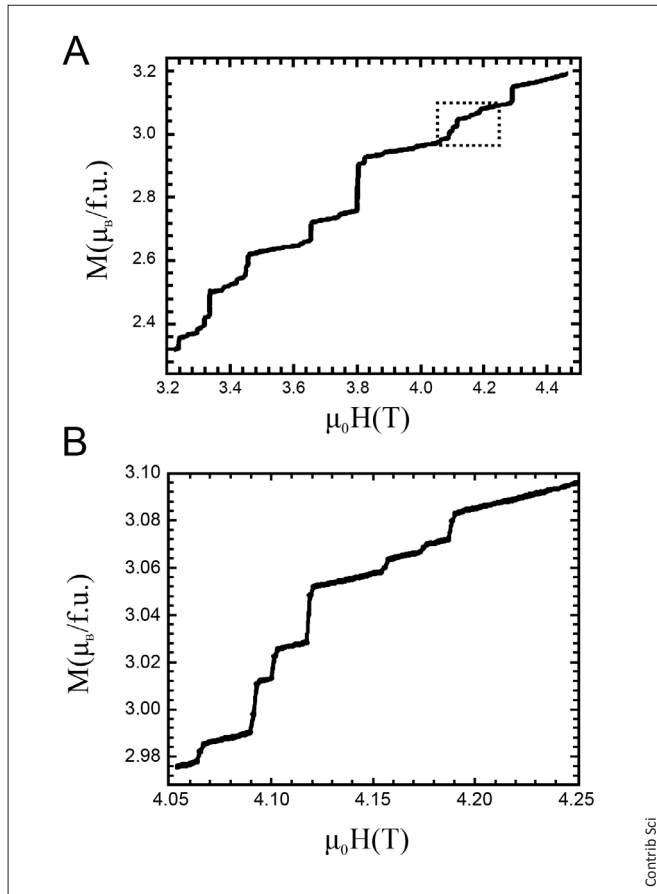


Fig. 3. Direct measurement of the avalanches in the hysteresis loop in a $\text{Pr}_{0.6}\text{Ca}_{0.4}\text{Mn}_{0.96}\text{Ga}_{0.04}\text{O}_3$ sample. The bottom panel shows an enlargement of the region indicated by the dotted rectangle. (From [9]).

Avalanche dynamics

In general, avalanches are microscopic and localized in small regions of the material. Direct measurement of the discontinuities in the hysteresis loops is difficult, but it has been achieved, for instance, in the case of ferromagnets [9]. An example is given in Fig. 3. More generally, avalanches are detected by experimental methods that are sensitive to the time derivative of the order parameter. In the case of ferromagnetic materials, fast variations of magnetization can be detected by measuring the induced voltage in a coil. The avalanches, in this case, produce so-called Barkhausen noise [7]. In the example of ferroelastic materials exhibiting structural FOPTs for which the order parameter is a component of the strain tensor, the avalanches can be detected by the acoustic emission technique [21], in which rapid variations of strain in certain regions of the material induce the emission of ultrasounds that can be detected on the surface by the appropriate transducers.

Figure 4 shows two examples of avalanches detected in ferromagnets [20] and ferroelastic materials. A similar behavior occurs in superconductors (vortex avalanches) [8] and ferroelectric materials (polarization avalanches). Avalanche sequences are often seen to be reproducible when the system is cycled many times through the transition. This indicates that the disorder is rather stationary (quenched disorder) and the system is highly athermal. However, as we discuss below, this is not always true.

The experimental observation that has allowed avalanche dynamics to be classified within the paradigm of out-of-equilibrium critical phenomena [19] is related to the statistical analysis of the properties of individual avalanches. For each jump event different properties can be measured, such as the amount of energy relaxed, the change in the order parameter, the duration of the avalanche, and the avalanche size. When these properties are measured for a large number of avalanches (for instance, those recorded during the whole transition), there is a significant difference compared to the statistics of standard measurements of physical properties. In general, due to the central limit theorem, the expectation is that the physical measurements will be Gaussian distributed, centered around an average value and with a certain standard deviation. However, avalanche properties are distributed according to probability densities with much fatter tails. Their distributions are typically described using a power-law probability density (Eq. 4):

$$p(x) \sim x^{-\alpha} \quad (4)$$

This indicates that the average values of such properties are meaningless in characterizing the system (i.e., they depend on the observation window) and that the only characteristic parameter is the power-law exponent α . Examples of such distributions for the case of Barkhausen noise in ferromagnets [6] or acoustic emission in ferroelastic materials [5] are shown in Fig. 5. Note that different materials exhibit the same values of the power-law exponents (universality) and that families (or classes) of materials can be identified.

This lack of characteristic scales indicates that systems displaying avalanche dynamics diverge in their spatial and/or temporal correlations, overriding any other microscopically relevant scale. This is a clear indication that, in a generalized parameter space (using renormalization group language), the systems are located in the close vicinity of a dynamic critical point and the critical exponents are expected to be universal.

This hypothesis has been reinforced in studies of the evolution of the avalanche size distribution when some athermal

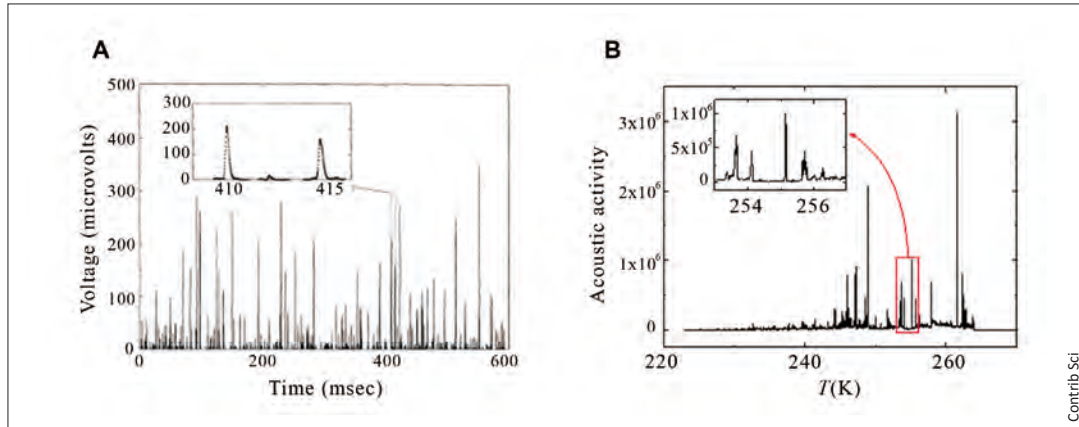


Fig. 4. Indirect measurement of avalanches by (A) Barkhausen noise detection in a ferromagnetic transition in a Fe-Ni-Co alloy [20] and (B) acoustic emission detection in a ferroelastic (martensitic) transition in a Cu-Zn-Al alloy.

ferroelastic systems are cycled many times across a FOPT [14]. An example of the experimental results obtained with a Cu-Al-Mn alloy exhibiting a structural phase transition is shown in Fig. 6. For some of these materials, the disorder (dislocations, etc.) is not totally quenched in. When the system is driven through the transition, simultaneous with the avalanche response, the disorder is slightly modified. Thus, the avalanche sequences are not exactly reproducible when one cycle is compared to the next. It has been observed that as-cast samples that cross the FOPT for the first time do not

exhibit a power-law distribution of avalanche sizes, but rather an exponentially dampened distribution (Eq. 5):

$$p(x) \sim x^{-\alpha} e^{-\beta x} \quad (5)$$

In the subsequent cycles through the transition, the cut-off parameter λ evolves towards zero, as shown in Fig. 6. After a certain number of cycles, the system reaches the true power-law distribution of avalanches characterized by the exponent α , which becomes quite stable. In other words,

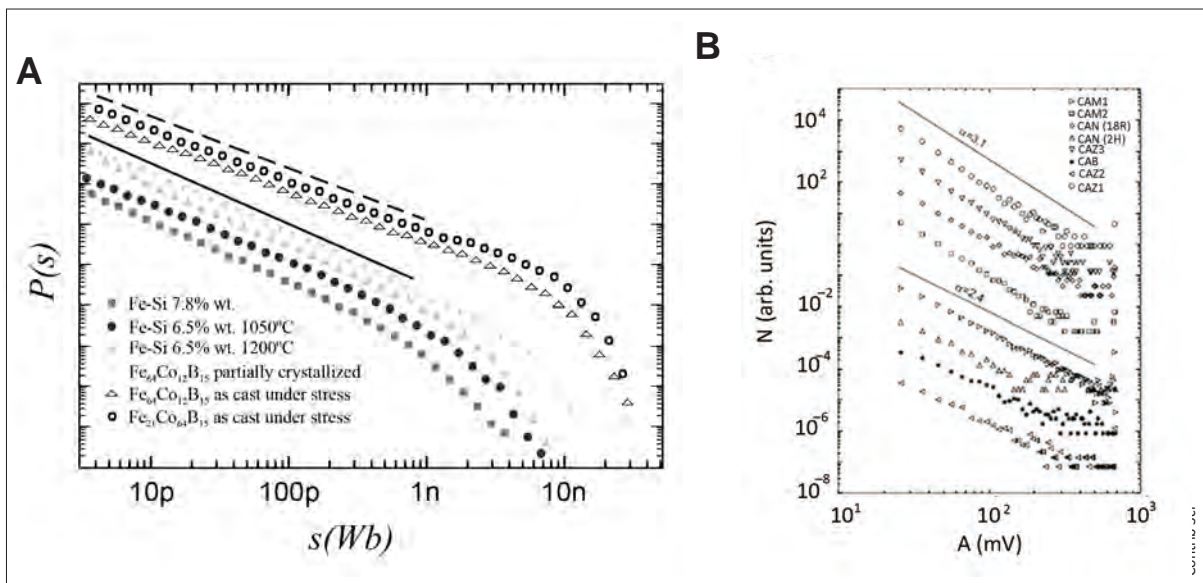


Fig. 5. Distribution of avalanche sizes in (A) ferromagnetic transitions [6] and (B) ferroelastic (martensitic) transitions [5]. The histograms, in log-log scale, show the lack of a characteristic scale (power-law behavior). The data were obtained from different alloys and thus reveal a certain degree of universality.

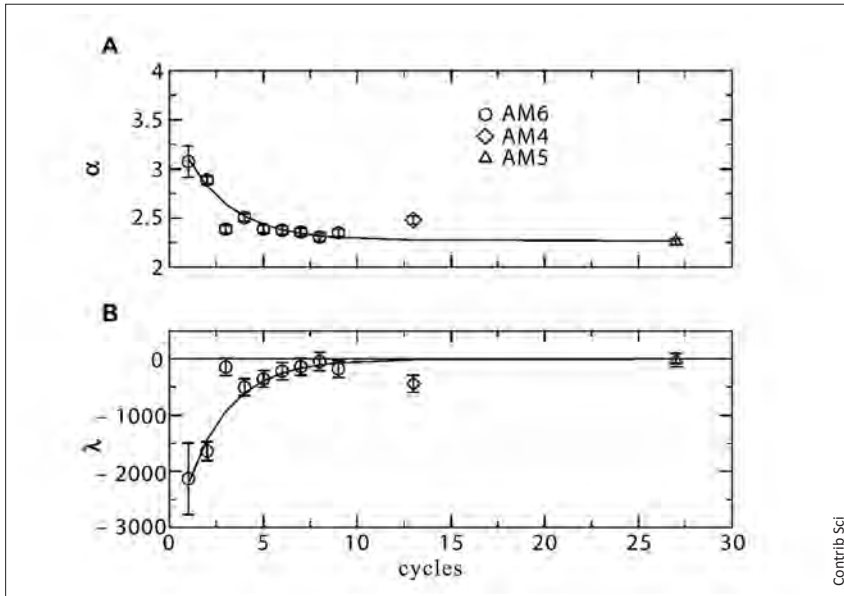


Fig. 6. Power-law exponent α and the exponential correction parameter λ for a Cu-Al-Mn alloy [14] as a function of the number of cycles through the ferroelastic (martensitic) transition. The data show the evolution of the disorder towards a self-organized situation, in which avalanches are power-law distributed ($\lambda = 0$).

during the first few cycles, the system self-organizes its disorder and finds an optimal non-equilibrium path (avalanche sequence) that exhibits “critical” properties. This confirms the attractive character of the “critical” state.

Models

Apart from the above-mentioned thermodynamic description in terms of macroscopic variables (M) or mesoscopic fields [$m(x)$], a number of microscopic models of avalanche dynamics within FOPT have been proposed. The first was the random field Ising model (RFIM) with athermal dynamics, introduced by J.P. Sethna and co-workers for the study of hysteresis and metastability [17]. The RFIM is a modification of the standard ferromagnetic Ising model with an external field (H) that describes a FOPT. On the sites of a regular lattice spin variables, S_i , are defined whose values are ± 1 . The Hamiltonian of the system is:

$$H = -\sum_{i,j}^{n,n} S_i S_j - H \sum_i S_i - \sum_i h_i S_i \quad (6)$$

where the first sum extends over all the pairs of nearest neighbors.

Apart from the first two standard terms in Eq. (6), there is a new, last term that accounts for the local quenched disorder [Gaussian-distributed quenched random fields h_i], and the use of zero-temperature local relaxation dynamics. This is an athermal mechanism for the relaxation of the model when

H is varied; it consists of flipping spins individually, as soon as they decrease the energy of the system. The model has been solved numerically within the mean-field approximation, using Bethe lattices, for different spatial dimensions and via Renormalization Group approaches. Some details are still not fully understood, but the model well describes the occurrence of avalanche dynamics and the critical power-law distribution of avalanche sizes [18]. After the RFIM was introduced, other models, including nucleation and the growth of many coexisting domains, were formulated, with similar properties [22].

Another set of models, focusing on the dynamics of a unique interface that separates the stable from the metastable phase, has been proposed. These models, designed to understand many out-of-equilibrium systems, collect ideas from the study of the pinning-depinning transitions of an elastic line and the self-organized criticality theory proposed by P. Bak [1]. In these models, the external field (H) provides the main driving force, but it should be compensated for by the elastic terms, which tend to reduce the interface curvature and the pinning forces due to the interaction of the interface with the local quenched disorder.

The main difference between these interface dynamics models and the RFIM is that, in the former, the avalanches turn out to be “critical” (power-law distributed) irrespective of the amount of disorder, whereas for the RFIM the system becomes critical only for a precise value of disorder (critical disorder).

Finally, it should be noted that none of these microscopic

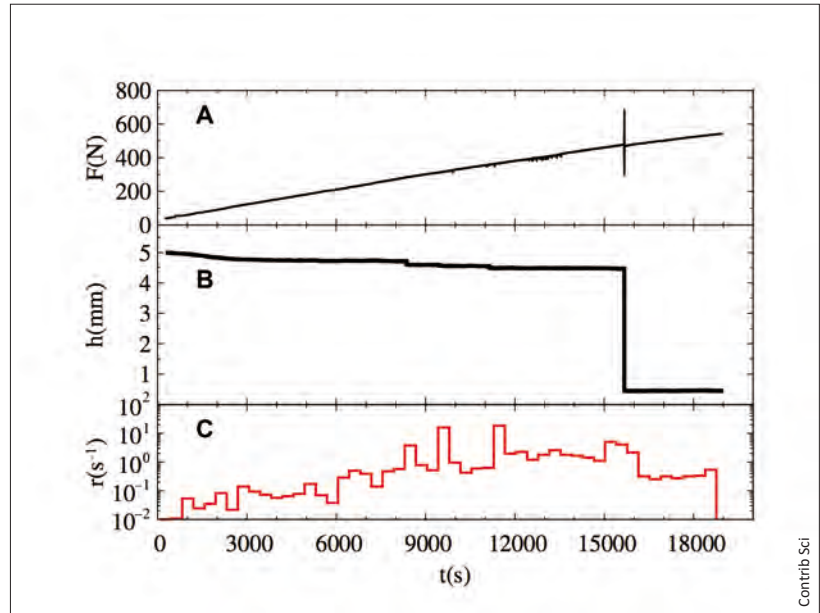


Fig. 7. Experimental results corresponding to the uniaxial compression of a porous SiO_2 sample (Vycor). (A) Force vs. time, (B) sample height vs. time, and (C) acoustic emission activity rate (in events per seconds). Note the logarithmic scale in the bottom panel.

models is able to account for the self-organization in the evolution of disorder. Only very recently, Pérez-Reche and collaborators [15,16] were able to unify the above-mentioned models and to offer an explanation for the evolution towards a critical self-organized path.

Porous materials under compression

In general, material fracture under external stress cannot be explained by the paradigm of FOPT and does not show avalanche dynamics. One of the main difficulties is that, because fracture is irreversible, it is difficult to identify concepts such as an underlying equilibrium free energy, metastability, and hysteresis in the process. Nevertheless, in the case of heterogeneous materials (amorphous materials, porous materials, granular materials, etc.) recent work [4] has demonstrated the importance of models for dynamic phase transitions. It is not our aim to discuss this topic here, but we will show that, in the case of highly porous materials, failure under compression does indeed exhibit avalanche dynamics and that this process has many similarities with other non-equilibrium failure processes, including earthquakes. Thus, avalanche dynamics could be a very general paradigm for understanding the physical mechanisms behind processes at very different scales.

The failure of porous materials under compression has recently received much attention, due to its relevance in forecasting the collapse of natural and artificial structures,

whether mines, buildings, or bones. Because material failure is heralded by precursor activity, interest lies in whether or not this activity can be used for prediction. Laboratory experiments have been carried out using many natural minerals and artificial materials. Here we describe, as an example, the results reported for Vycor [2,11], a material that consists of an interconnected quartz skeleton (SiO_2) with 40% porosity. The average pore diameter is < 10 nm.

Materials at room temperature are placed between two plates and a compressional force is applied. The experiment can be optionally performed by imposing a lateral pressure or by controlling the speed of the plates (strain driven) or the force rate (stress driven). Here we focus on stress-driven experiments without lateral pressure. Acoustic emission sensors are embedded in the compression plates and detect ultrasonic events, just as seismographs detect earthquakes.

Figure 6 shows a typical experiment using Vycor. While the force is monotonously increased, the length of the sample, measured by a laser extensometer, decreases in intermittent steps until a large drop occurs, corresponding to the failure of the sample. Acoustic emission activity (number of detected events per unit time) exhibits peaks of high activity not totally correlated with the decreases in sample height. The random process is therefore not homogeneous in time, but has a rate that varies from 10^{-2} to 10^3 events per second. Furthermore, acoustic activity continues after sample collapse, indicating that the behavior of the material's debris is similar to that of the intact sample. Events (avalanches) are

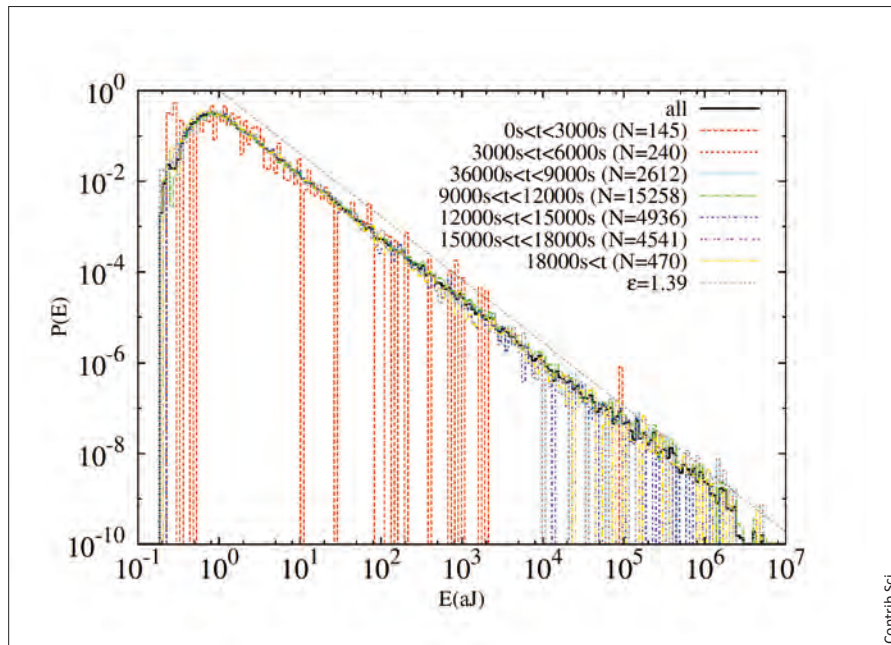


Fig. 8. Distribution of avalanche energies for the experiment shown in Fig. 7. The different histograms correspond to different time windows, as indicated by the legend. The data show the robust power-law behavior (lack of characteristic scale), extending 5–6 decades and independent of the analysed time window.

separated by waiting periods that range from 10^{-4} to 10^5 s. Analysis of the energies of each single event shows a power-law distribution of energies (Eq. 7):

$$p(E) \sim E^{-\varepsilon} \quad (7)$$

that spans eight orders of magnitude, as shown in Fig. 7. Despite the fact that the avalanche rate fluctuates enormously, the distribution $p(E)$ is quite stationary and has a very well-determined exponent ($\varepsilon = 1.39$). Thus, the intermittent failure processes exhibit a lack of characteristic scales that allows them to be classified as an example of avalanche dynamics.

As mentioned above, the statistics of acoustic emission events exhibit many similarities with those of seismological problems. The power-law distribution of energies, despite the large differences in energy scales, is nothing more than a Gutenberg–Richter law describing earthquake magnitude. However, the similarities go far beyond this distribution. Statistical techniques for the analysis of waiting times, correlations between avalanches, and the existence of aftershocks have revealed unexpected equivalences between the two phenomena. This opens up the possibility that an under-

standing of the avalanche dynamics during the compression of porous materials in the lab (labquakes) may, in the future, improve our understanding of earthquakes in the Earth's crust. ■

Acknowledgements. The authors acknowledge the Spanish Ministry of Economy and Competitiveness for financial support (grant numbers MAT2013-40590-P and MAT2015-69777-REDT).

Competing interests. None declared.

References

1. Bak P, Tang C, Wiesenfeld K (1987) Self-organized criticality: An explanation of the $1/f$ noise. *Phys Rev Lett* 59:381 doi:10.1103/PhysRevLett.59.381
2. Baró J, Corral A, Illa X, Planes A, Salje EKH, Schranz W, Soto-Parra DE, Vives E (2013) Statistical similarity between the compression of a porous material and earthquakes. *Phys Rev Lett* 110:088702 doi:10.1103/PhysRevLett.110.088702
3. Bertotti G (1998) *Hysteresis in magnetism: for physicists, materials scientists and engineers*. Academic Press, London, UK doi:10.1016/S0042-207X(99)80004-9

4. Bonamy D, Bouchaud E (2011) Failure of heterogeneous materials: a dynamic phase transition? *Phys Rep* 498:1-44 doi:10.1016/j.physrep.2010.07.006
5. Carrillo L, Mañosa L, Ortín J, Planes A, Vives E (1998) Experimental evidence for universality of acoustic emission avalanche distributions during structural transitions. *Phys Rev Lett* 81:1889 doi:10.1103/PhysRevLett.81.1889
6. Durin G, Zapperi S (2000) Scaling exponents for barkhausen avalanches in polycrystalline and amorphous ferromagnets. *Phys Rev Lett* 84:4705 doi:10.1038/nphys1884
7. Durin G, Zapperi S (2006) The Barkhausen effect. In: Bertotti G, Mayergoyz ID (eds) *The Science of hysteresis*, Vol. II:181-267. Academic Press, Oxford, UK
8. Field S, Witt J, Nori F, Ling X (1995) Superconducting vortex avalanches. *Phys Rev Lett* 74:1206 doi:10.1103/PhysRevLett.74.1206
9. Hardy V, Majumdar S, Lees MR, Paul DMcK, Yaicle C, Hervieu M (2004) Power-law distribution of avalanche sizes in the field-driven transformation of a phase-separated oxide. *Phys Rev B* 70:104423 doi:10.1103/PhysRevB.70.104423
10. Lifshitz EM, Pitaevskii LP (1976) *Landau and Lifshitz course of theoretical physics*. Vol. 5, *Statistical Physics*, 3rd ed., part 1, Chapter XIV, Pergamon Press, Oxford, UK
11. Nataf GF, Castillo-Villa PO, Baró J, Illa X, Vives E, Planes A, Salje EKH (2014) Avalanches in compressed porous SiO₂-based materials. *Phys Rev E* 90:022405 doi: 10.1103/PhysRevE.90.022405
12. Papon P, Leblond J, Meijer PHE (2006) *The physics of phase transitions*. 2nd edition, Springer Verlag, Berlin, Heidelberg, Germany ISBN-10 3-540-33389-4
13. Pérez-Reche FJ, Vives E, Mañosa L, Planes A (2001) Athermal character of structural phase transitions. *Phys Rev Lett* 87:195701 doi:10.1103/PhysRevLett.87.195701
14. Pérez-Reche FJ, Stipcich M, Vives E, Mañosa L, Planes A, Morin M (2004) Kinetics of martensitic transitions in Cu-Al-Mn under thermal cycling: Analysis at multiple length scales. *Phys Rev B* 69:064101 doi:10.1103/PhysRevB.69.064101
15. Pérez-Reche FJ, Truskinovsky L, Zanzotto G (2007) Training-induced criticality in martensites. *Phys Rev Lett* 99:075501 doi:10.1103/PhysRevLett.99.075501
16. Pérez-Reche FJ, Truskinovsky L, Zanzotto G (2008) Driving-induced crossover: from classical criticality to self-organized criticality. *Phys Rev Lett* 101:230601 doi:10.1103/PhysRevLett.101.230601
17. Sethna JP, Dahmen K, Kartha S, Krumhansl JA, Roberts BW, Shore JD (1993) Hysteresis and hierarchies: Dynamics of disorder-driven first-order phase transformations. *Phys Rev Lett* 70:3347 doi:10.1103/PhysRevLett.70.3347
18. Sethna JP, Dahmen KA, Myers CR (2001) Crackling noise. *Nature* 410:242-250 doi:10.1038/35065675
19. Sornette D (2000) *Critical phenomena in natural sciences*. Springer Verlag, Berlin, Germany doi:10.1007/3-540-33182-4
20. Urbach JS, Madison RC, Markert JT (1995) Interface depinning, self-organized criticality, and the Barkhausen effect. *Phys Rev Lett* 75:276 doi:10.1103/PhysRevLett.75.276
21. Vives E, Ortín J, Mañosa L, Ràfols I, Pérez-Magrané R, Planes A (1994) Distributions of avalanches in martensitic transformations. *Phys Rev Lett* 72:1694 doi:10.1103/PhysRevLett.72.1694
22. Vives E, Goicoechea J, Ortín J, Planes A (1995) Universality in models for disorder-induced phase transitions. *Phys Rev E* 52:R5 doi:10.1103/PhysRevE.52.R5
23. Yeomans JM (1992) *Statistical mechanics of phase transitions*. Oxford Science Publications, Clarendon Press, Oxford, UK doi:10.1080/00107517808210882

About the image on the first page of this article. This photograph was made by Prof. Douglas Zook (Boston University) for his book *Earth Gazes Back* [www.douglaszookphotography.com]. See the article "Reflections: The enduring symbiosis between art and science," by D. Zook, on pages 249-251 of this issue [http://revistes.iec.cat/index.php/CtS/article/view/142178/141126]. This thematic issue on "Non-equilibrium physics" can be unloaded in ISSUU format and the individual articles can be found in the Institute for Catalan Studies journals' repository [www.cat-science.cat; http://revistes.iec.cat/contributions].